Cell. Mol. Biol. (ISSN: 1165-158X)

Journal Homepage: www.cellmolbiol.org

Cellular and Molecular Biology

Original Article

Anti- COVID-19 drug discovery by flavonoid derivatives: an extensive computational drug design approach

Subhasis Banerjee[1], Souvik Mukherjee[2], Mohsin Kazi[3], Kalyan Kumar Sen[2], Arka Das[4], Raquibul Hasan[5], Yuan-Seng Wu[6,7], Aziz Eftekhari[8,9], Sreemoy Kanti Das[10], Mohammad Nur-e-Alam[11], Md. Moklesur Rahman Sarker[12,13*], Mohd Fahami Nur Azlina[14*]

[1] Division of Pharmaceutical Chemistry, Eminent College of Pharmaceutical Technology, Moshpukur, Barbaria, Barasat, 24 PGS(N), Kolkata-700126, West Bengal, India
[2] Division of Pharmaceutical Technology, Gupta College of Technological Sciences, Ashram More, Asansol, 713301 West Bengal, India
[3]Department of Pharmaceutics, College of Pharmacy, King Saud University, P.O. Box 2457; Riyadh 11451, Saudi Arabia
[4]Department of Pharmaceutical Chemistry, Acharya and BM Reddy College of Pharmacy, Soldevanahalli, Bengaluru, 560107 Karnataka, India
[5]Department of Pharmaceutical Sciences, College of Pharmacy, Mercer University, Atlanta, GA 30341, United States
[6]Sunway Microbiome Centre, School of Medical and Life Sciences, Sunway University, Selangor 47500, Malaysia
[7] Department of Biological Sciences, School of Medical and Life Sciences, Sunway University, Selangor 47500, Malaysia
[8]Department of Biochemistry, Faculty of Science, Ege University, Izmir 35040, Turkey
[9]Department of Life Sciences, Western Caspian University, Baku AZ1072, Azerbaijan
[10]Department of Pharmacology, Faculty of Pharmacy, Lincoln University College, Malaysia
[11]Department of Pharmacognosy, College of Pharmacy, POBOX-2457, King Saud University, Riyadh 11451, KSA
[12]Department of Pharmacy, Gono University (Bishwabidyalay), Nolam, Mirzanagar, Savar, Dhaka- 1344, Bangladesh
[13]Pharmacology and Toxicology Research Division, Health Med Science Research Network, 3/1 Lalmatia, Dhaka 1207, Bangladesh
[14]Department of Pharmacology, Faculty of Medicine, University Kebangsaan Malaysia, Jalan Yacob Latif, Kuala Lumpur 56000, Malaysia

Article Info

Article history:

Received: September 05, 2023
Accepted: April 09, 2024
Published: August 31, 2024

Use your device to scan and read the article online

Abstract

The present study deals with the in-silico analyses of several flavonoid derivatives to explore COVID-19 through pharmacophore modelling, molecular docking, molecular dynamics, drug-likeness, and ADME properties. The initial literature study revealed that many flavonoids, including luteolin, quercetin, kaempferol, and baicalin may be useful against SARS β-coronaviruses, prompting the selection of their potential derivatives to investigate their abilities as inhibitors of COVID-19. The findings were streamlined using in silico molecular docking, which revealed promising energy-binding interactions between all flavonoid derivatives and the targeted protein. Notably, compounds 8, 9, 13, and 15 demonstrated higher potency against the coronavirus Mpro protein (PDB ID 6M2N). Compound 8 has a -7.2 Kcal/mol affinity for the protein and binds to it by hydrogen bonding with Gln192 and π-sulfur bonding with Met-165. Compound 9 exhibited a significant interaction with the main protease, demonstrating an affinity of -7.9 kcal/mol. Gln-192, Glu-189, Pro-168, and His-41 were the principle amino acid residues involved in this interaction. The docking score for compound 13 is -7.5 Kcal/mol, and it binds to the protease enzyme by making interactions with Leu-41, π-sigma, and Gln-189. These interactions include hydrogen bonding and π-sulfur. The major protease and compound 15 were found to bind with a favourable affinity of -6.8 Kcal/mol. This finding was further validated through molecular dynamic simulation for 1ns, analysing parameters such as RMSD, RMSF, and RoG profiles. The RoG values for all four of the compounds varied significantly (35.2–36.4). The results demonstrated the stability of the selected compounds during the simulation. After passing the stability testing, the compounds underwent screening for ADME and drug-likeness properties, fulfilling all the necessary criteria. The findings of the study may support further efforts for the discovery and development of safe drugs to treat COVID-19.

Keywords: Flavonoids, Pharmacophore, Drug-likeliness, MD simulation, Molecular docking, Molecular dynamic, ADMET.

1. Introduction

Viruses are always the primary cause of a large number of newly emerging and reemerging diseases, which puts human and animal health at serious risk. They are a consi-

∗ Corresponding author.
E-mail address: moklesur2014@gmail.com, moklesur2002@yahoo.com (Md. M. R. Sarker); nurazlinamf@ukm.edu.my (M. F. Nur Azlina).
Doi: http://dx.doi.org/10.14715/cmb/2024.70.8.5

derably greater global concern in the developing world, particularly when it comes to public health, than they have been in the last century. Pathogenic viral infections are the primary cause of the most serious and fatal human diseases. These viruses spread quickly and significantly increase the global burden of morbidity and mortality [1]. A hospital in Wuhan, Hubei Province, China, grabbed attention from across the world on December 31st when it reported several patients who had pneumonia with no known cause. In this situation, China banned the whole region in early 2020 to halt the spread of a new coronavirus strain known as severe acute respiratory syndrome coronavirus-2, and the world took note (SARS-CoV-2) [2]. It quickly had the entire planet under its control, like a monstrous serpent. On January 30, 2020, the World Health Organisation (WHO) declared this epidemic a public health emergency of worldwide significance. However, more people are being affected by SARS-CoV-2 compared to other viruses such as MERS-CoV (34.4%) and SARS-CoV (9.19%), leading to an increasing problem of community transmission [3]. On July 16th, 2020, the WHO reported that there had been more than 13,338,364 confirmed cases worldwide, resulting in at least 57,931 deaths. SARS-CoV-2, like MERS-CoV and SARS-CoV, is a member of the coronavirus family, particularly the β-coronavirus family [4].

SARS-CoV-2, a single-stranded RNA virus, efficiently leverages host systems to perform a variety of physiological functions, such as viral entry, assembly, subsequent viriogenesis, and even genomic replication and protein synthesis. This achievement finally leads to the host's pathological demise [5]. Hence, by considerably enhancing any of the aforementioned viral life cycle events with tiny compounds or short chains of amino acids, vaccinations may significantly benefit the host. With all these aims, the researchers are trying to find the juggernaut in a reasonable amount of time. Only at the end of 2020 will the vaccine be ready for widespread distribution, so it is essential to find approved experimental treatments and off-label medications, as well as antiviral phytochemicals, to combat SARS-CoV-2 infection. Choosing the conventional approach will take years to generate a lead, whereas various structure-based modelling techniques (macromolecule or ligand), repurposing the existing antiviral based on their respective background research, and rapid drug database screening may prove to be the most effective strategies to speed up the development of novel inhibitors against SARS-CoV-2 [6]. However, only a few potential new drugs show promise in combating this serious threat. Researchers discovered that Nafamostat, a powerful MERS-CoV membrane fusion inhibitor, prevents SARS-CoV-2 infection [7]. As an anti-protozoal, nitazoxanide has a variety of antiviral effects [8]. Compared to Nafamostat, its effectiveness against 2019nCoV infection was more encouraging [9]. Wang et al. discovered Favipiravir, Ribavirin, and Penciclovir with substantial anti-COVID-19 properties while evaluating a series of known antiviral nucleoside analogues. Anecdotal information on the use of protease inhibitors (Pit) during the early stages of this outbreak spurred the study of this medication. During that process, healthcare providers administered some of the first-line anti-HIV medications, such as lopinavir/ritonavir, remdesivir, and tipranavir, to treat this infection [10]. However, it remains unclear whether the medication class specifically suited to the HIV structure would initially exhibit sufficient cross-reactivity to effectively combat SARS-CoV-2. Since the beginning of time, the plant kingdom has continuously provided the human race with a vast array of medicinally significant phytoconstituents. Plant-based antivirals are not brand new.

According to the annual report on medicinal chemistry, seven out of ten synthetic antivirals that the FDA approved between 1984 and 1995 were based on a natural product template [10]. Food plants include many flavonoids, which disrupt the NLRP3 signalling pathway. Flavonoids such as luteolin, myricetin, apigenin, quercetin, kaempferol, and baicalin have been shown to be effective against SARS beta coronaviruses. The respiratory agony syndrome associated with SARS coronaviruses is reported to develop in part as a result of viral activation of the NLRP3 inflammasome, which increases the production of inflammatory cytokines. They fight viruses in several ways [11].

These biomarkers and their semi-synthetic analogues effectively treat the target virus. The scientific community has already acknowledged the major Pit Mpro, also known as 3CLpro, as the preferred target due to its usefulness in processing viral polyproteins [12]. The molecular docking technique has beecome popular for the designing of possible potential drug candidates for different emerging diseases [13-15]. The molecular docking strategy and technique was used in the current study to model a few commercially available flavonoids that could potentially interact with the primary Pit for the treatment of COVID-19. Frequently, a sizable pool of compounds fails to pass all drug discovery hurdles because they do not adhere to safety and drug-likeness standards. As a result, the rate of failure can be significantly decreased at the design stage before moving on to the wet stage, which also makes the entire drug development process more cost-effective. The current work therefore aims to find the drug resemblance and pharmacokinetic properties of the docked compounds produced from natural flavonoids, as well as the binding poses.

2. Materials and Methods

2.1 Pharmacophore modeling and database searching

Pharmacophores interact favorably with a macromolecule and enable a ligand to correctly occupy the active site of a biological target, leading to an acceptable therapeutic effect. The three-dimensional spatial layout of the interlocking functional groups necessary for its action is established by pharmacophore modelling (PCM). Due to the importance of phytoconstituents in the treatment of viral infection, we chose baicalein, catechin, kaempferol, and naringenin as the four commercially available flavonoids for a ligand-based PCM experiment [16]. We performed PCM using Pharma Gist, an internet web server [17]. The researchers first drew the 2D structures of these four compounds using ChemSketch and then saved them in the mol2 format using Open Babel software [18]. Pharma Gist was then used to import all these compounds and generate their common 3D properties. Using Pymol as a molecular viewer, Figure 1 illustrates the examination of the pharmacophore model made up of all typical flavonoids [19]. The common features so obtained are 2 H-bond donors, 1 H-bond acceptor, and three aromatic centers. The 3D features thus obtained were further transferred to another web server called ZincPharmer, which utilises its search

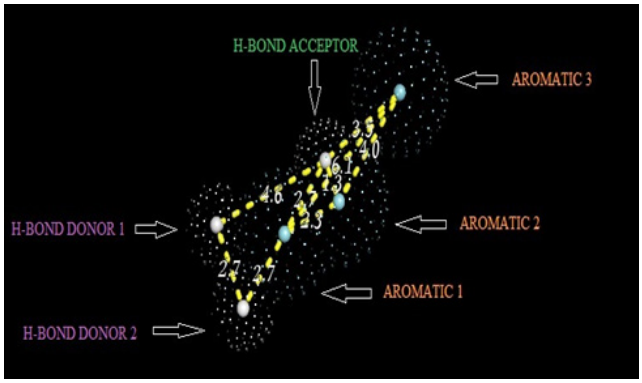

Fig. 1. Common pharmacophoric features of standard flavonoids Baicalein, Catechin, Kaempferol and Naringenin.

engine the Zinc database to generate a huge number of hits bearing nearly the same pharmacophoric features [20]. A set of 10 compounds with a root mean square deviation (RMSD) of less than 0.57 were selected for additional research from many hits. While designing a second batch of ten compounds [11-20], we considered the pharmacophoric characteristics of both the standards and the compounds retrieved from the zinc database. All the 20 compounds thus obtained were docked against Mpro of SARS-CoV-2, owing to their importance in the present research.

2.2 Protein modeling

A fresh crystal structure of the Coronavirus Mpro protein (PDB entry number 6M2N) was imported from the Protein Data Bank (PDB, http://www.rcsb.org). Its PDB entry number is 6M2N, and it has a 2.20 resolution. It also complexes with the inhibitor baicalein by using an HP laptop with a 1.7 GHz central processing unit, four GB of RAM, and Windows 7, a 32-bit operating system [21]. We used MGL Tools 1.5.6 to model the protein. We deleted the first heteroatoms, which included the cocrystal occupying the substrate binding site and the water molecules. We employed the energy-minimization method to fix the process's coordinate deviation using the Swiss PDB reader [22]. Next, we examined the energy-minimized protein using the Python Molecular Viewer. In the end, missing and polar hydrogens were merged, incomplete Gasteiger atomic charges were added, and bond ordering was assigned. All the protein's atoms were converted to Autodock4 type (t) and the pdb file was modified to pdbqt, where q stands for charge and t for Autodock4 type, in order to make the protein compatible with docking software.

2.3 Ligand modeling

Using the free software ACD ChemSketch, the 2D structures of all the compounds (1–20) were created. All the 2D structures were converted to 3D using the PRODRG web server [23]. The resulting 3D structures were stored in protein data bank (PDB) form. All the compounds underwent additional processing in the same way as the protein before saving them in "pdbqt" form. The standards also underwent this adjustment. Supplementary Table 1 (Table S-1) displays the 2D structures of all the ligands taken into consideration for this in silico analysis.

2.4 Validation of molecular docking

To guarantee the dependability and reproducibility of the docking process, validation is a crucial step. Redocking the ligand already present at the active site accomplishes this step. The extraction of the co-crystal 3WL (Baicalein) from the protein's co-crystallized structure (PDB: 6M2N) emptied the active site. We then redocked the co-crystal inside the protein's active site. There is excellent agreement between the inhibitor's position during docking, 3WL, and the protein structure. RMSD determined the redocked conformation and unprocessed crystallographic conformation of Compound 3WL. By reproducing the experimentally observed binding mechanism for the viral major protease, the docking approach is guaranteed to be reliable.

2.5 Molecular docking studies

The primary objective of the molecular docking technique is to make an informed prediction regarding the composition of the ligand-receptor complex through the utilization of computational approaches. The docking process encompasses two distinct yet interdependent steps. Firstly, it involves sampling several conformations that the ligand can adopt when bound to the protein's active site. Secondly, it entails the classification of these residues based on a performance index. By executing these intricately woven steps, molecular docking sheds between ligands and receptors are performed, unravelling the prediction of their interactions and aiding drug discovery and design endeavors. The Auto Dock Vina application was employed to accomplish molecular docking [24]. During molecular docking studies, the grid box coordinates were strategically set to cover both the entire protein and the site of interest, ensuring accurate ligand placement. The grid centre points were set to X = − 36.403, Y = − 56.315, and Z = 41.288, and given these requirements, the grid box occupied the active site in such a way that all the crucial amino acid residues for the active site were located inside the box. For each docked molecule, docking yields nine major conformers. The conformer chosen for the next investigation was considered the most active against the viral major protease due to its superior docking pose and lowest binding energy. The interaction study of bound complex structures was conducted using the PyMol molecular viewer and the BIOVIA Discovery Studio programme.

2.6 Drug-likeness studies

Any chemical that possesses specific active functional groups can interact with a protein; however, due to noncompliance with the Lipinski and Veber rules, they frequently struggle to be a candidate to seek. The specifications that must be met while creating a medication are laid forth by these guidelines. The virtual experiment of the drug-likeness study is now crucial to take into account when constructing virtual bioactives. In the current investigation, there are no exceptions. Any breach of the aforementioned rules led to the removal of the compound from the research. The study showed that the compound, which was removed due to a breach of the rules, had no effect on the major protease of SARS-CoV-2. The study was carried out using an internet web server named Swiss ADME [22].

2.7 ADME Profiling

Sometimes, despite obtaining a thumbs up from the drug-likeness study, a molecule cannot be optimised due to a subpar pharmacokinetic profile. Hence, if virtual pharmacokinetic screening can be performed at the early stages

Table 1. Twenty (20) compounds' docking output and drug-likeness research.

Docking Score	Druggability Parameters (Drug-Likeliness)								
Compound	**BE***	**Mol wt (g/mol)**	**Consensus Log P**	**H-bond donors**	**H-bond acceptors**	**Lipinski's Rule**	**Rotatable bonds**	**TPSA[α]**	**Veber's Rule**
Co-crystal (Baicalein)	-7.8	270	2.68	3	5	No	1	91	No
Standard 1 (Catechin)	-7.5	290	1.37	5	6	No	1	110	No
Standard 2 (Kaempferol)	-7.8	285	2.17	4	6	No	1	114	No
Standard 3 (Naringenin)	-7.5	272	2.12	3	5	No	1	90	No
1	-7.4	286	3.48	2	5	No	0	74	No
2	-7.9	288	2.39	2	6	No	0	92	No
3	-7.8	303	1.82	4	7	No	0	118	No
4	-7.4	275	2.65	3	9	No	0	90	No
5	-7.5	429	3.43	4	11	1 violation HBA>10	4	158	1 violation TPSA>140
6	-7.9	354	3.48	4	8	No	3	131	No
7	-6.9	310	1.91	4	6	No	1	98	No
8	-7.2	302	2.03	3	7	No	1	95	No
9	-7.9	330	2.13	3	7	No	2	95	No
10	-7.2	372	3.98	2	5	No	4	67	No
11	-7.5	417.29	4.46	3	3	No	7	70.59	No
12	-7.0	417.29	4.45	3	3	No	7	70.59	No
13	-7.5	429.53	1.85	2	7	No	6	104.48	No
14	-7.3	400.96	4.11	1	3	No	5	52.01	No
15	-6.8	469.60	2.04	2	6	No	9	105.22	No
16	-8.6	587.62	5.92	3	7	2 violation (MW>500) (Log P>5)	11	122.16	1 violation (Rot bonds>10)
17	-8.7	429.85	4.81	1	4	No	4	72.44	No
18	-7.3	358.48	0.45	3	6	No	7	71.86	No
19	-7.6	372.87	4.45	2	3	No	7	109.14	No
20	-7.7	391.47	2.01	0	4	No	4	63.37	No

* Binding energy or docking score in Kcal/mol

[α] Topological polar surface area in $Å^2$

of drug discovery, it can lessen the financial burden on the company by reducing the number of compounds that need to be optimized. The ADME prediction research facilitates the rapid creation of safe medications. The goal of this in-silico study is to identify the most active compounds among all the actives extracted during primary screening by focusing on a few ADME characteristics that all active molecules should meet. The pharmacokinetic studies of each ligand must be determined significantly earlier in the lead optimisation stage using computer-aided drug design (CADD), which is the sole method. This ADME profiling was maintained in the current investigation as part of secondary screening, as opposed to the initial active screening, which was based on drug-likeness, docking score, and posture. ADME investigations were carried out by the Swiss ADME online web server [25-27].

2.8 MD simulation analysis of potential derivatives

Investigational ligand-protein binding mode was carried out by using LARMD server [28]. The LARMD server was fed the protein-ligand complex in PDB format as it was obtained experimentally. Water was used as an explicit model with a molecular dynamic time of 1 ns. Afterwards, after delineating reaction coordinates, all relevant input files for MD simulation were submitted. The work was renamed, and a new job was posted. A software called initialization was used to get the sequence data in order to find the nonstandard residue(s). The four chemicals under consideration for more research were all chosen for the energy computation and trajectory analysis. All nonstandard residues' force fields were produced. The recommended tunnel was chosen for simulation for the Int mod module. The residues that make up the catalytic domain of the proteins were analyzed for their residence time in contact with all the selected ligands in order to calculate their % occupancy for interaction throughout the simulation exercise. The simulation trajectory, the RMSD, and the radius of gyration (Rg) of the qualifying compounds were all calculated and analyzed. For the purposes of analysing RMSD, Rg, and Root Mean Square Fluctuation (RMSF), the Cpptraj module of the AMBER16 software was employed [29]. The binding free energy (Gbind) was computed using the MM/PBSA and MM/GBSA techniques utilising the enthalpy or total energy of the system (E) and the system's solvation entropy (TS).

3. Results

Creating the safest Pit against COVID-19 infection was the aim of the current study. Flavonoids were chosen as phytoconstituents with antiviral properties since they have been used to treat numerous viral diseases, including COVID-19. In order to identify the common chemical properties causing the interaction with the active site amino acid residues, four typical flavonoids of therapeutic value such as baicalein, catechin, kaempferol, and naringenin were first aligned using pharmacophore modelling. A total of twenty compounds were used, ten of which were taken from the zinc database and had similar pharmacophoric characteristics to standards, and the remaining ten were created using the pharmacophore established as shown in Figure 1. These twenty substances were taken into account for the next computational investigation, which includes molecular docking, drug-likeness, and an examination of the ADME profile. To find any worrying fragment from the substance under investigation, fragment alert data was also created. With Autodock Vina, all the compounds, including the standards, were docked correctly. Docking causes the ligand to take on various different postures. The bioactive position was chosen and processed for additional analysis based on which stance had the highest affinity or the lowest score or binding energy. The following analysis featured drug-likeness research, which examined adherence to a set of guidelines put out by two outstanding scientists, Lipinski and Veber. The major criterion for excluding a drug from the ADME profile check, the next stage of examination, was continued to be violation of any regulation. Both Veber's parameter and Lipinski's Rule of Five were used to estimate the drug-like qualities, indicating that a significant number of compounds created by PCM were discovered to have unique features suitable for inclusion in the ADME prediction research. Lipinski's Rule of 5 asserts that a chemical must meet specific criteria established by those experts in order to be pharmacologically active. As the virus is mostly colonised in the lungs, compounds having TPSA values more than 90 Å^2, namely compounds 6, 7, 8, 9, 13, and 15, were taken into consideration for the pharmacokinetic investigation in order to prevent unfavourable CNS effects. The active site study identified His-41, Cys-44, Met-49, Leu-141, Asn-142, Gly-143, Ser-144, Cys-145, His-163, His-164, Met-165, Glu-166, Asp-187, Arg-188, and Gln-189 as the important amino acids implicated in ligand binding. The conformer produced by Autodock Vina with the lowest energy of all

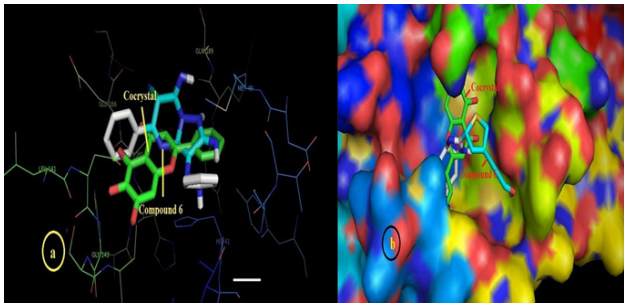

Fig. 2. (a) Stereo view demonstrating the strongest conformer of chemical 6 overlaid on the native co-crystal at the active site of the coronavirus major protease. (b)Molecular surface image of compound 6 at its ideal position.

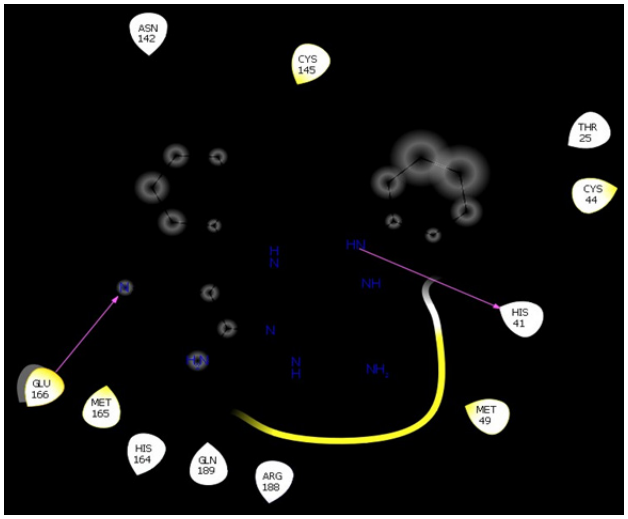

Fig. 3. 2D interactions of compound 6 with the active site residues of coronavirus Mpro.

the docked compounds was taken into account. The drug likelihood information and the docking output are included in Table 1. A significant interaction between compound 6 and the major protease was identified, with an affinity of -7.9 Kcal/mol. Together with two -cation interactions with His-41 and Met-49, it specifically created two hydrogen bonds with Glu-166 and Cys-45. As demonstrated in Figures 2 and 3, two -alkyl interactions with Asn-142 and Leu-27 were also noticed.

As seen in Figures 4 and 5, compound 7 formed many contacts during docking with the primary protease, including stacking with His-41, hydrogen bonding with Thr-190, and Sulphur interactions with Cys-44 and Met-49. This resulted in a binding energy of -6.9 Kcal/mol.

It can be seen from Figure 6 and 7, that compound 8 interacts with the protein with an affinity of -7.2 Kcal/mol by establishing hydrogen bond with Gln192, π-sulfur bonding with Met-165.

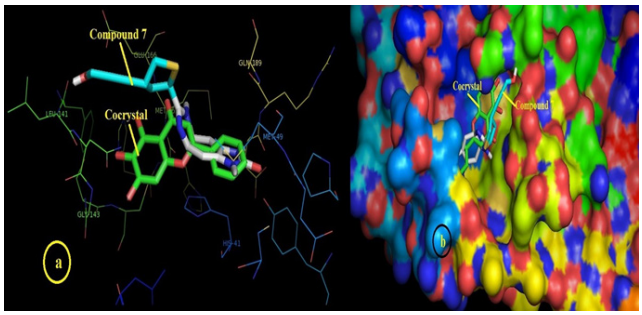

Fig. 4. (a) A stereo view of the best conformer of compound 7, which is in the active site of the main protease of the coronavirus, is shown by placing it on the co-crystal. (b) molecular surface view of the compound's best pose is also presented.

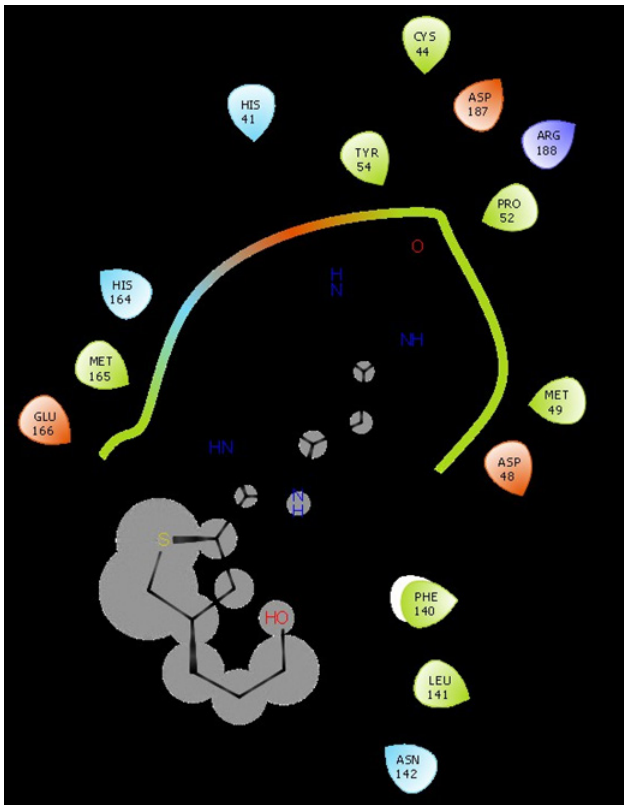

Fig. 5. The two-dimensional structure of the interactions between the best conformer of compound 7 and the active site of the coronavirus MPro is shown.

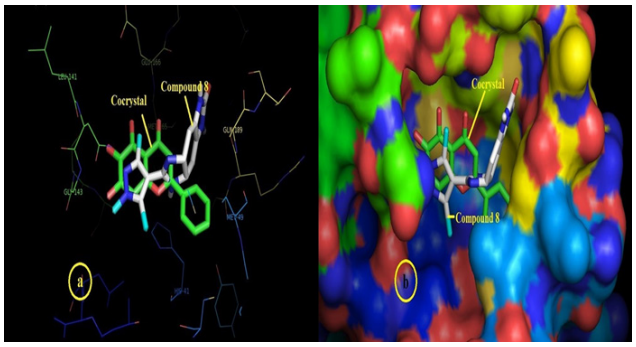

Fig. 6. Docking semblance of compound 8. **a** 3D Spatial arrangement of the best conformer (most stable) of compound 8 within the binding site of coronavirus main protease, aligning with the original co-crystal. **b** Molecular surface view of the best-fitted posture of compound 8.

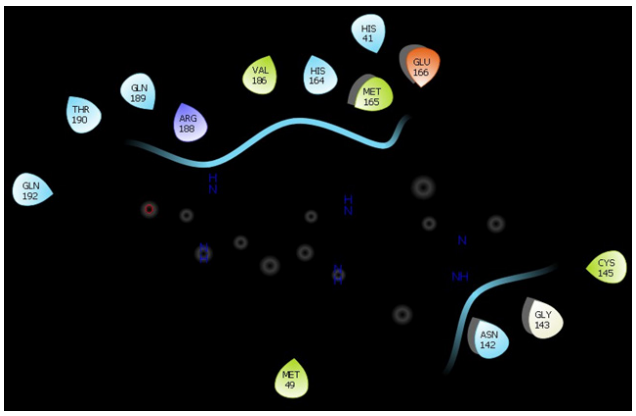

Fig. 7. The best conformer of compound 8 interacts in two dimensions with the coronavirus Mpro active site residues.

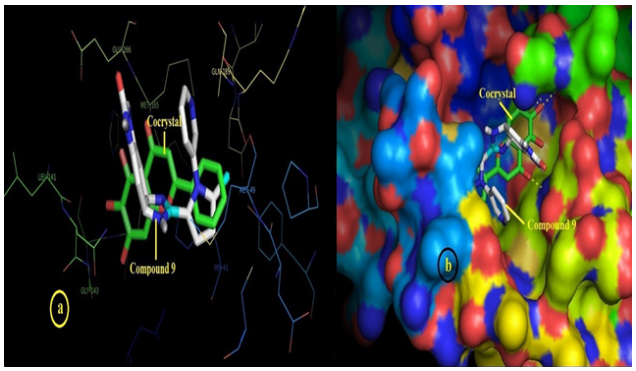

Fig. 8. (a) Docking pose of compound 9 & (b) Molecular surface view of compound 9.

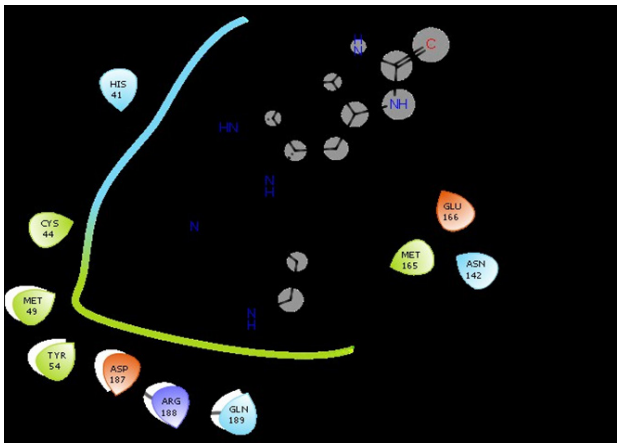

Fig. 9. 2D connections of the finest conformer of compound 9 with active site residues of coronavirus Mpro.

A prominent interaction between compound 9 and the main protease was observed with an affinity of -7.9 kcal/mol. The principle amino acid residues involved in this interaction were found to be Gln-192, Glu-189, Pro-168, His-41 as shown in Figures 8 and 9.

Compound 13 binds with the protease enzyme through docking score of -7.5 Kcal/mol by establishing interactions, like hydrogen bonding with Leu-41, π-sigma, π-sulfur with Gln-189 and His-41 respectively as shown in Fig. 10. More interestingly, a salt bridge was also found with Glu-166 as observed in Figure 11.

The major protease and compound 15 were found to bind with a favorable affinity of -6.8 Kcal/mol, as illustrated in Figure 12 and 13.

All of these substances have significant potential to be taken into consideration for the following stage of research, i.e., ADME prediction, since they are all well ascribed to having drug-like qualities without breaking either Lipinki's Rule of Five or Veber's rule [30]. Compounds 16 and 17 did not make it into the final position of prediction despite having the greatest binding energies, -8.6 Kcal/mol and -8.7 Kcal/mol, respectively. Compound 16 exhibits several infractions of both criteria for drug-like qualities, but compound 17, which had a value of less than 90 and was CNS vulnerable, was unable to maintain the momentum. Compounds 1, 10, 11, 12, 14, 18, and 20 are among the other compounds that must overcome a similar challenge. All of these compounds had protease affinities that were within the acceptable range of -7.0 to -7.7 Kcal/mol. The SARS-CoV-2 Mpro was used to scan the binding pattern of these pharmacophore-derived drugs, and the results showed that hydrogen bonding interaction was the primary factor in binding. The amount of exploration depends on how flexible a ligand is, which is determined by the presence of rotatable bonds. Compounds 2, 3, and 4 were excluded from the ADME investigation because they lacked rotatable bonds.

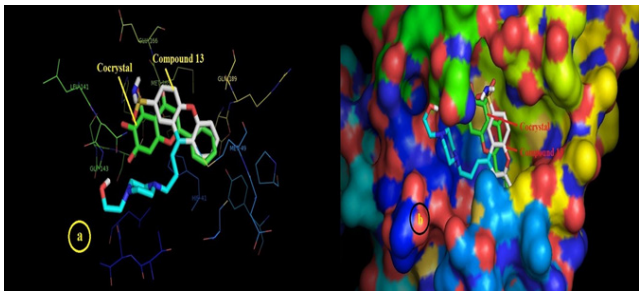

Fig. 10. (a) Docking pose of compound 13 & (b) Molecular surface view.

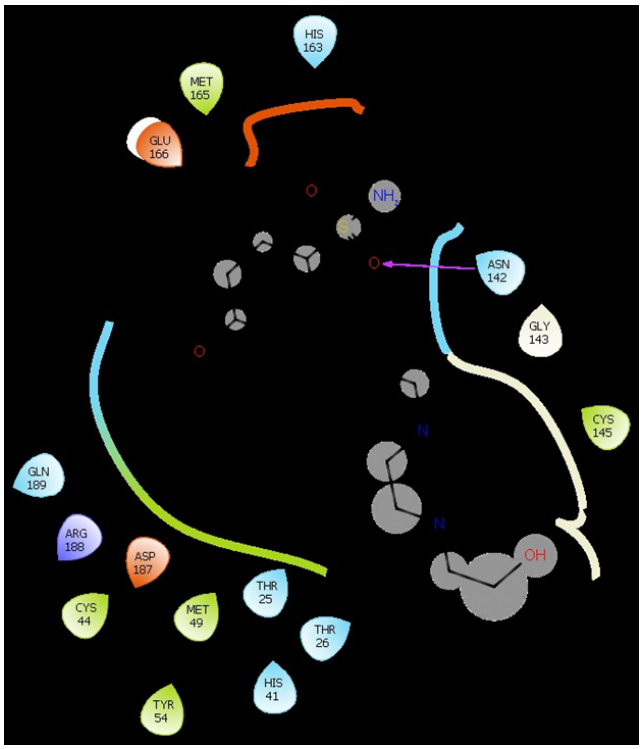

Fig. 11. Two-dimensional docking pose of compound 13.

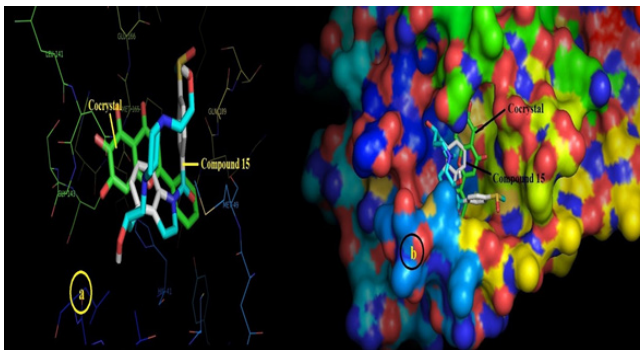

Fig. 12. Docking semblance of compound 15. **a** 3D Spatial arrangement of the best conformer (most stable) of compound 15 within the binding site of coronavirus main protease, aligning with the original co-crystal. **b** Molecular surface view of the best-fitted posture of compound 15.

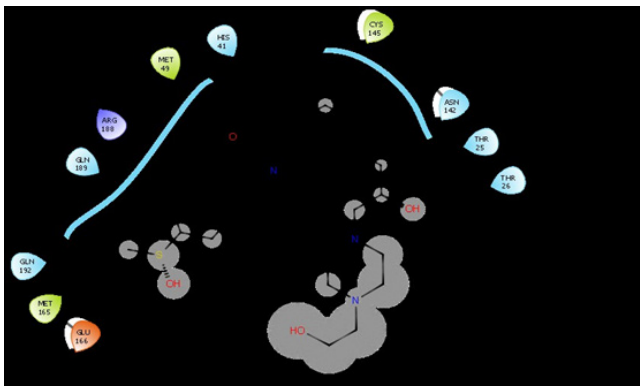

Fig. 13. Best docking 2D pose of compound 15 with the proximally placed binding site residues of Mpro.

For the ADME prediction investigation, the compounds (6, 7, 8, 9, 13 and 15) that were screened from the docking and drug-like tests underwent further evaluation. The blood-brain barrier's (BBB) permeability is one of the factors considered for ADME profiling. Although the central nervous system (CNS) is not where protease inhibitors are intended to stay, any peripherally acting drugs with BBB permeability might nonetheless have a negative effect on the CNS [31]. Since they can quickly pass the viral barrier and may easily infiltrate the intestinal tract, molecules with high gastrointestinal (GI) permeability can make medications that are taken orally accessible. Skin permeability (log Kp) values that are more negative indicate that the chemicals have a harder time penetrating the skin membrane [32]. Cytochrome P450 (CYP450) isoenzymes family play a vital part in metabolic biotransformation. Drug-drug interactions may be eliminated if these CYP450 enzymes are inhibited since this metabolic acti-

Table 2. ADME profiling of screened compounds.

No	Log S* (ESOL)	GI absorption	BBB permeant	Log K_p [α]	CYP450 inhibition					Medicinal Chemistry alerts	
					1A2	2C19	2C9	2D6	3A4	PAINS[µ]	Brenk[€]
6	M. Sol	Low	No	-6.09	Yes	No	Yes	No	No	1	1
7	Sol	High	No	-7.48	Yes	No	No	No	No	0	1
8	Sol	High	No	-7.11	Yes	No	No	No	No	0	0
9	Sol	High	No	-7.21	Yes	No	No	Yes	No	0	0
13	Sol	High	No	-7.8	No	No	No	Yes	No	0	0
15	Sol	High	No	-8.12	No	No	No	Yes	No	0	0

Table 3. The selected bioactive compounds' binding free energy (in kcal/mol).

Name of compound	Free energy (kcal/mol)	Main protease
8	MM/PBSA	-10.33
	MM/GBSA	-12.93
9	MM/PBSA	-5.79
	MM/GBSA	-13.28
13	MM/PBSA	-3.34
	MM/GBSA	5.04
15	MM/PBSA	-4.4
	MM/GBSA	0.56

vity will be reduced [33]. Drug or metabolite accumulation brought on by declining clearance values may result in a number of toxicities in the body [34]. The investigation was further enhanced by the generation of structural warning data, which may quickly detect the toxicophoric point in a molecule. These two remarkable characteristics, known as Brenk alert and In the early phases of drug discovery, pan-assay interference compounds (PAINS) alert examine the desired compounds in a way that allows any major region to be rapidly ruled out [35]. The majority of PAINS are chemically promiscuous, exhibiting binding affinity for a range of targets regardless of the target that has been specified, resulting in false positives and unexpected results. The findings of the ADME studies on the six most important active chemicals are shown in Table 2.

To guarantee their safety, the predicted ADME profile was further validated on each of the six initially selected compounds. Certain standards were maintained for the final screening of qualifying compounds. The substances must not inhibit three or more CYP450 isoenzymes, and last but not least, not trigger pain or Brenk alarms. The ADME study's findings, which fall far within the acceptable limit, show that compounds 8, 9, 13, and 15 are the safest of all. Due to both of the other two compounds, 6 and 7, carrying Brenk Alert, they were unable to advance to the final selection. No particular medications or vaccines are effective against any of the corona viruses, target-specific drug research is of utmost relevance. From the beginning of time, the plant kingdom has continuously provided the scientific community with a variety of parent products, whose systemic modelling led to the synthesis of several synthetic antivirals. In light of the aforementioned information, we generated a few molecules based on a pharmacophore created by aligning four common flavonoids. We have produced a few protease inhibitors by properly utilising a few computational technologies. since most currently utilised COVID-19 medications largely target the viral primary protease. Most of the substances fit into the primary protease's binding pocket effectively, supporting the pharmacophore and future design. However, in order to guarantee that the important interactions are undamaged, molecular dynamic modelling will need to be performed in the future. Due to their strict adherence to medication-like features and ADME profile, four out of the 20 compounds (8, 9, 13, and 15) emerged as suitable candidates to deal with. Four compounds were identified as the most promising ones based on an overall analysis of docking and ADME research. Research using molecular dynamic modelling was done using all these bioactive

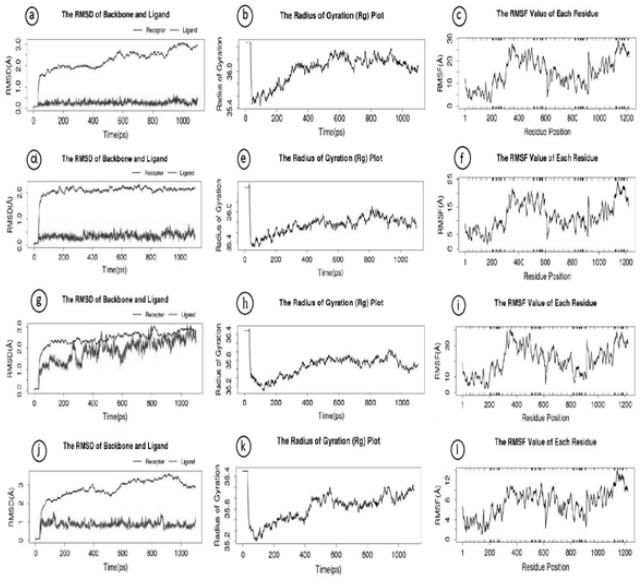

Fig. 14. Molecular Dynamic Simulations of all the four active compounds; a, d, g, j: RMSD (Root Mean Square Deviation) diagram of compounds 8, 9, 13, 15; b, e, h, k: Rg (Radius of gyration) plots of compounds 8, 9, 13, 15; c, f, i, l: RMSF (Root Mean Square Fluctuation) values and its corresponding graph of compounds 8, 9, 13, 15.

substances. According to Table 3, all four of these compounds had effective binding affinities with the enzyme based on their MM/PBSA and GBSA scores.

Furthermore, the chosen compounds' corresponding motion could change the adaptability, conformation, and capabilities of the proteases, as demonstrated by the molecular analysis of the ligand protein interactional binding mode based on MD simulations (Str mod) with external forces applied on the ligand. (Figure 14.).

To ascertain the stability of the interaction between the protein-ligand complex, a 1000 ps long MD simulation was run in the condition of water solvation. The MD trajectory's stability was confirmed using RMSD and Rg. The COVID-19 main protease's mean RMSDs of CA atoms lie between 0 to 3, according to the results shown in Figure 14(a, d, g, j)). Figure 14(b, e, h, and k) shows that the Rg values for all four of the compounds varied significantly (35.2–36.4).

The distribution of the ligand may have a considerable impact on the internal atomic fluctuation of the protein. As all four complexes are effectively aligned with the majority of the target protein amino acids, this is evident in the RMSF plot of all four complexes.

While the other three complexes show larger fluctuation RMSF values well up to 30, the Root Mean Square Fluctuations (RMSF) per amino acid of compound 15-main protease complex (Figure 14.) in a regular fluctuation pattern between 2 and 12. The target protein's structural flexibility was severely impacted, as seen by the RMSD, Rg, and RMSF data. This could be as a result of the chemicals' proximity to the proteases' internal core. Any of the evaluated substances might have an impact on the conformational dynamics of the target protein under simulation. As a result, the functional characteristic and its inherent capacity for generating a clinical condition brought on by the corona virus might change. The current research shows that newly created chemicals, which are derived from a pharmacophore created from flavonoids, may significantly block the corona virus's primary protease and can be produced synthetically as antivirals to effectively stop the spread of this serious threat.

4. Discussion

Computational screening-based drug design investigations of designed derivatives of flavonoid for the identification of potent drugs for COVID-19 had been conducted meticulously, each result demonstrated well to explain its importance. Molecular modelling techniques such as Molecular docking and Molecular dynamic simulation had demonstrated the interaction with significant residues and stability of the docked derivatives structures with selected protein. With the coronavirus Mpro protein (6M2N), Gln192 and π-sulfur bonding with Met-165 residues make contacts with Compound 8, Gln-192, Glu-189, Pro-168, and His-41 with compound 9 and Leu-41, π-sigma, and Gln-189 with compound 13. The best-bounded conformations were further subjected to the deep-down analysis of MD simulations. The stability of the virtual hit molecules (08,09,13 and 15) with the receptor protein is important, hence the average values for each Molecular Dynamic simulation analysis were noted to determine the fluctuation of results concerning binding stability with the target, and overall results are quite acceptable, thus deemed to be stable structures. Further wet laboratory experimental analysis is required to validate the computational hypothetical results to confirm the inhibitory character against the COVID-19. ADME profile estimations for potential virtual hit molecules (08, 09, 13 and 15) were additionally conducted to evaluate the drug-likeness activity of the selected derivatives, each compound had presented acceptable chemical and physical properties (Tables 1 and 2). Hence, this *In silico* study could be a roadmap to propose COVID-19 antiviral drugs with the best bounded aspects within enzyme pocket as well as good medicinal chemistry and bioavailability estimations.

5. Conclusion

With its widespread disease, fatalities, and interruptions to normal life, the COVID-19 pandemic undoubtedly had a significant effect on the world. It can be challenging to adequately treat patients who have the virus because of the severe lack of appropriate drugs, which is a serious problem. As no particular medications or vaccines are effective against any of the corona viruses, target-specific drug research is of utmost relevance. From the beginning of time, the plant kingdom has continuously provided the scientific community with a variety of parent products, whose systemic modelling led to the synthesis of several synthetic antivirals. In light of the aforementioned information, we generated a few molecules based on a pharmacophore created by aligning four common flavonoids. As the bulk of presently used COVID-19 drugs primarily target the viral main protease, we developed a few protease inhibitors by effectively utilising a few computational methods, such as docking studies, drug-likeness, and Pharmacokinetic profile check. Most of the substances fit into the primary protease's binding pocket effectively, supporting the pharmacophore and future design. For the MD simulation research that ensures intact main contacts, four out of the twenty compounds (8, 9, 13, and 15) were taken into further consideration, notably for compound 15. Due to their strict adherence to drug-like features and ADME profile, these four compounds have become promising candidates to deal with. Finally, it is important to note that classical bioinformatics, when properly combined with chemo-informatics methods, produced fresh data for SARS-CoV-2 research at a breakneck pace.

Abbreviation

COVID-19: Coronavirus disease-19; ADME: Absorption, distribution, metabolism and excretion; MD Simulation: Molecular docking simulation; SARS-CoV-2: severe acute respiratory syndrome coronavirus-2; MERS-CoV: Middle East respiratory syndrome coronavirus; HIV: Human immunodeficiency virus; FDA: Food and drug administration; NLRP3: nucleotide-binding domain, leucine-rich–containing family, pyrin domain–containing-3; PCM: Pharmacophore modelling; RMSD: Root mean square deviation; PDB: Protein Data Bank; PAINS: Pan-assay interference compounds; CYP450: Cytochrome P450; RMSF: Root mean square fluctuations.

Conflicts of interest

The authors declare no that they do not have any financial or intellectual conflict of interest.

Consent for publications

All authors have read and agreed to publish the manus-

cript.

Ethics approval and consent to participate
No ethical issue for this publication as no human or animals were used in the present research.

Informed consent
Informed consent is not applicable for this article as no patient or parcipant was involved in the study.

Availability of data and material
The authors declare that they have embedded all the data in the manuscript. However, for further queries on data and any kind of question regarding this manuscript will be available in contact with the corresponding authors.

Authors' contributions
SB conceptualized, designed the study, and interpreted the results. SM, KKS, AD, and Y-SW created data. SB, SM, KKS and AD analyzed and interpreted data and presented the data in tables and figures. SB and SM wrote the manuscript. MK, RH, Y-SW, AE, "SKD, MNA, MMRS, and MFNA critically reviewed and edited the manuscript. MMRS revised the final manuscript. MMRS and MFNA supervised the project. All authors read the manuscript and agreed to be accountable for all aspects of the work and approved the final manuscript.

Funding
The study was supported by King Saud University (Researchers Supporting Project Number RSPD2024R994) and Universiti Kebangsaan Malaysia (Approval code: FF-2020-016).

Acknowledgements
The authors would like to extend their sincere appreciation to the Researchers Supporting Project Number (RSPD2024R994), King Saud University, Riyadh, Saudi Arabia. The author also thankful to the Faculty of Medicine, Universiti Kebangsaan Malaysia for providing support to this project (Approval code: FF-2020-016).

References

1. Akash S, Bibi S, Yousafi Q, Ihsan A, Mustafa R, Farooq U et al (2023) Ligand-based drug design of Pinocembrin derivatives against Monkey-Pox disease. Arab J Chem 16(11): 105241. doi: 10.1016/j.arabjc.2023.105241
2. Wang C, Horby PW, Hayden FG, Gao GF (2020) A novel coronavirus outbreak of global health concern. The lancet 395(10223): 470-473. doi: 10.1016/S0140-6736(20)30185-9
3. Mahase E (2020) Coronavirus: covid-19 has killed more people than SARS and MERS combined, despite lower case fatality rate. BMJ 368: m641. doi: 10.1136/bmj.m641
4. Chan JF-W, Yuan S, Kok K-H, To KK, Chu H, Yang J, Xing F, Liu J, Yip CC, Poon RWS, Tsoi HW et al (2020) A familial cluster of pneumonia associated with the 2019 novel coronavirus indicating person-to-person transmission: a study of a family cluster. The lancet 395(10223): 514-523. doi: 10.1016/S0140-6736(20)30154-9
5. Subissi L, Imbert I, Ferron F, Collet A, Coutard B, Decroly E et al (2014) SARS-CoV ORF1b-encoded nonstructural proteins 12–16: replicative enzymes as antiviral targets. Antivir Res 101(1): 122-130. doi: 10.1016/j.antiviral.2013.11.006
6. Liu C, Zhou Q, Li Y, Garner LV, Watkins SP, Carter LJ et al (2020) Research and development on therapeutic agents and vaccines for COVID-19 and related human coronavirus diseases. ACS Cent Sci 6(3): 315-331. doi: 10.1021/acscentsci.0c00272
7. Li G, De Clercq E (2020) Therapeutic options for the 2019 novel coronavirus (2019-nCoV). Nat Rev Drug Discov 19(3): 149-150. doi: 10.1038/d41573-020-00016-0
8. Odhar HA, Ahjel SW, Albeer AA, Hashim AF, Rayshan AM, Humadi SS et al (2020) Molecular docking and dynamics simulation of FDA approved drugs with the main protease from 2019 novel coronavirus. Bioinformation 16(3): 236. doi: 10.6026/97320630016236
9. Yamamoto M, Matsuyama S, Li X, Takeda M, Kawaguchi Y, Inoue J et al (2016) Identification of nafamostat as a potent inhibitor of Middle East respiratory syndrome coronavirus S protein-mediated membrane fusion using the split-protein-based cell-cell fusion assay. Antimicrob Agents Chemother 60(11): 6532-6539. doi: 10.1128/aac.01043-16
10. Rossignol JF (2014) Nitazoxanide: a first-in-class broad-spectrum antiviral agent. Antivir Res 110(1): 94-103. doi: 10.1016/j.antiviral.2014.07.014
11. El Sayed KA (2000) Natural products as antiviral agents. Stud Nat Prod Chem 24(1): 473-572. doi: 10.1016/S1572-5995(00)80051-4
12. Wang M, Cao R, Zhang L, Yang X, Liu J, Xu M et al (2020) Remdesivir and chloroquine effectively inhibit the recently emerged novel coronavirus (2019-nCoV) in vitro. Cell Res 30(3): 269-271. doi: 10.1038/s41422-020-0282-0
13. Akash S, Hossain A, Mukerjee N, Sarker MMR, Khan MF, Hossain MJ, Rashid MA, Kumer A, Ghosh A, León-Figueroa DA, Barboza JJ, Padhi BK, Sah R et al (2023) Modified coptisine derivatives as an inhibitor against pathogenic *Rhizomucor miehei*, *Mycolicibacterium smegmatis* (Black Fungus), Monkeypox, and Marburg virus by molecular docking and molecular dynamics simulation-based drug design approach. Front Pharmacol 14(4): 1140494. doi: 10.3389/fphar.2023.1140494.
14. Akash S, Aovi FI, Azad MA, Kumer A, Chakma U, Islam MR et al (2023) A drug design strategy based on molecular docking and molecular dynamics simulations applied to development of inhibitor against triple-negative breast cancer by Scutellarein derivatives. PLoS ONE 18(10): e0283271. doi: 10.1371/journal.pone.0283271
15. Akash S, Bibi S, Biswas P, Mukerjee N, Khan DA, Hasan MN et al (2023) Revolutionizing anti-cancer drug discovery against breast cancer and lung cancer by modification of natural genistein: an advanced computational and drug design approach. Front Oncol 13: 1228865. doi: 10.3389/fonc.2023.1228865
16. Sayed SB, Nain Z, Khan MSA, Abdulla F, Tasmin R, Adhikari UK et al (2020) Exploring lassa virus proteome to design a multi-epitope vaccine through immunoinformatics and immune simulation analyses. Int J Pept Res Ther 26: 2089-2107. doi: 10.1007/s10989-019-10003-8
17. McKee DL, Sternberg A, Stange U, Laufer S, Naujokat CJ et al (2020) Candidate drugs against SARS-CoV-2 and COVID-19. Pharmacol Res 157: 104859. doi: 10.1016/j.phrs.2020.104859
18. Zhang L, Liu Y (2020) Potential interventions for novel coronavirus in China: A systematic review. J Med Virol 92 (5): 479-490. doi: 10.1002/jmv.25707
19. Yang SY (2010) Pharmacophore modeling and applications in drug discovery: challenges and recent advances. Drug Discov Today 15(11-12): 444-450. doi: 10.1016/j.drudis.2010.03.013
20. Schneidman-Duhovny D, Dror O, Inbar Y, Nussinov R, Wolfson HJ (2008) PharmaGist: a webserver for ligand-based pharmacophore detection. Nucleic Acids Re 36 (2): W223-W228. doi:

10.1093/nar/gkn187
21. O'Boyle NM, Banck M, James CA, Morley C, Vandermeersch T, Hutchison GR et al (2011) Open Babel: An open chemical toolbox. J Cheminform 3(33): 1-14. doi: 10.1186/1758-2946-3-33
22. DeLano WL (2002) Pymol: An open-source molecular graphics tool. CCP4 Newsl. Protein Crystallogr 40(1): 82-92. http://www.ccp4.ac.uk/newsletters/newsletter40/11_pymol.pdf
23. Irwin JJ, Shoichet BK (2005) ZINC− A free database of commercially available compounds for virtual screening. J Chem Inf Model 45(1): 177-182. doi: 10.1021/ci049714+
24. Kuzikov M, Costanzi E, Reinshagen J, Esposito F, Vangeel L, Wolf M et al (2021) Identification of inhibitors of SARS-CoV-2 3CL-pro enzymatic activity using a small molecule in vitro repurposing screen. Pharmacol Transl Sci 4(3): 1096-1110. doi: 10.1021/acsptsci.0c00216
25. Akash S, Bayıl I, Hossain MS, Islam MR, Hosen ME, Mekonnen AB et al (2023) Novel computational and drug design strategies for inhibition of human papillomavirus-associated cervical cancer and DNA polymerase theta receptor by Apigenin derivatives. Sci Rep 13(1): 16565. doi: 10.1038/s41598-023-43175-x
26. Akash S, Bayıl I, Mahmood S, Mukerjee N, Mili TA, Dhama K et al (2023) Mechanistic inhibition of gastric cancer-associated bacteria Helicobacter pylori by selected phytocompounds: A new cutting-edge computational approach. Heliyon 9 (10): 1-22. doi: 10.1016/j.heliyon.2023.e20670
27. Akash S, Hosen ME, Mahmood S, Supti SJ, Kumer A, Sultana S et al (2023) Anti-parasitic drug discovery against Babesia microti by natural compounds: an extensive computational drug design approach. Front Cell Infect Microbiol 13: 1222913 doi: 10.3389/fcimb.2023.1222913
28. Guex N, Peitsch MC (1997) SWISS-MODEL and the Swiss-Pdb Viewer: an environment for comparative protein modeling. Electrophoresis 18 (15): 2714-2723. doi: 10.1002/elps.1150181505
29. Van Aalten DM, Bywater R, Findlay JB, Hendlich M, Hooft RW, Vriend GJ et al (1996) PRODRG, a program for generating molecular topologies and unique molecular descriptors from coordinates of small molecules. J Comput Aided Mol Des 10(6): 255-262. doi: 10.1007/BF00355047
30. Trott O, Olson AJ (2010) AutoDock Vina: improving the speed and accuracy of docking with a new scoring function, efficient optimization, and multithreading. J Comput Chem 31(2): 455-461. doi: 10.1002/jcc.21334
31. Yang JF, Wang F, Chen YZ, Hao GF, Yang GF (2020) LARMD: integration of bioinformatic resources to profile ligand-driven protein dynamics with a case on the activation of estrogen receptor. Brief Bioinformatics 21(6): 2206-2218. doi: shttps://doi.org/10.1093/bib/bbz141
32. Roe DR, Cheatham III TE (2013) PTRAJ and CPPTRAJ: software for processing and analysis of molecular dynamics trajectory data. J Chem Theory Comput 9(7): 3084-3095. doi: https://doi.org/10.1021/ct400341p
33. Daina A, Michielin O, Zoete VJ (2017) SwissADME: a free web tool to evaluate pharmacokinetics, drug-likeness and medicinal chemistry friendliness of small molecules. Sci Rep 7(1): 42717. doi: 10.1038/srep42717
34. Potts RO, Guy RH (1992) Predicting skin permeability. Pharm Res 9: 663-669. doi: 10.1023/A:1015810312465
35. Hollenberg PF (2002) Characteristics and common properties of inhibitors, inducers, and activators of CYP enzymes. Drug Metab Rev 34(1-2): 17-35. doi: 10.1081/DMR-120001387